

From Global to Local: Learning Context-Aware Graph Representations for Document Classification and Summarization

Ruangrin Ldallitsakool¹, Margarita Bugeño^{1,2}, Gerard de Melo^{1,2}

¹University of Potsdam, ²Hasso Plattner Institute (HPI)

ldallitsakool@uni-potsdam.de, {margarita.bugueno, gerard.demelo}@hpi.de

Abstract

This paper proposes a data-driven method to automatically construct graph-based document representations. Building upon the recent work of Bugeño and de Melo (2025), we leverage the dynamic sliding-window attention module to effectively capture local and mid-range semantic dependencies between sentences, as well as structural relations within documents. Graph Attention Networks (GATs) trained on our learned graphs achieve competitive results on document classification while requiring lower computational resources than previous approaches. We further present an exploratory evaluation of the proposed graph construction method for extractive document summarization, highlighting both its potential and current limitations. The implementation of this project can be found on GitHub¹.

1 Introduction

In recent NLP systems, documents are typically processed by language models (LMs) as linear sequences of tokens—such as characters, subwords, words, or sentences. While this sequential formulation allows models to capture token order, it often constrains their ability to represent long-range dependencies and higher-level document structures, particularly as input length increases (Hudson and Moubayed, 2022). Moreover, LMs frequently encounter redundancy, where similar or identical content recurs within or across documents (Ma et al., 2022), leading to inefficiencies in learning and representation as the model repeatedly encodes overlapping information.

One promising direction for effective and efficient document modeling lies in graph-based representations, where tokens are represented as nodes. Tokens referring to the same entity or exhibiting strong semantic similarity can be merged

into a single node, enhancing representational efficiency. Edges are then established between nodes—optionally encoding positional or syntactic relations—thereby capturing the document’s structural information and contextual dependencies.

Most research focuses on heuristically constructed graph representations, where node and edge features are manually designed based on task objectives or domain expertise, such as linguistic knowledge. However, designing effective graph representations remains challenging, as such approaches often struggle with domain transferability and depend heavily on external preprocessing steps (Bugeño and de Melo, 2023; Wang et al., 2024).

An automatic, data-driven graph construction approach, such as that described in Bugeño and de Melo (2025), could serve as a solution. Thus, this paper further advances automatically learned graph representations from attention models, with an emphasis on improving **local context awareness** and **computational efficiency**.

Our main contributions are threefold: (i) we extend the graph structure learning framework of Bugeño and de Melo (2025) by replacing full attention with sliding-window attention, substantially reducing computational requirements; (ii) we systematically evaluate multiple model configurations on two document classification benchmarks, achieving improved performance over prior results; and (iii) we study the applicability of our approach to extractive document summarization, a task that has been largely underexplored in previous work.

2 Related Work

2.1 Attention Mechanisms

To overcome the challenges in capturing semantic and structural dependencies in long document processing, state-of-the-art models such as Transformers (Waswani et al., 2017) have been extended. Notably, Beltagy et al. (2020) and Zaheer et al.

¹Project repository: <https://github.com/ida1r/SlidingWindowAttnGraphs>

(2020) introduced sparse attention mechanisms that extend the effective input length of Transformers while maintaining linear computational complexity. Their models, *Longformer* and *BigBird*, demonstrated superior results across a range of natural language processing (NLP) tasks.

Several sparse attention patterns have been proposed in their work. **Sliding window attention** employs a fixed-size window around each token. It was proposed to reduce computation, as well as an effective tool for context localization (Kovaleva et al., 2019). To further support mid-range context dependency, Beltagy et al. (2020) adapted **dilated sliding window attention** from dilated CNNs (Van Den Oord et al., 2016), to increase the window size without increasing the computational need. Zaheer et al. (2020) introduced **random attention**, which allows their model to expand and approximate the different contexts. Both works incorporate **global attention**, which aggregates the representation of a document on specially added or pre-selected tokens, to capture structural information and long-distance dependencies.

2.2 Traditional Graph-Based Representations

Graph models offer several advantages over sequential language models (Xu et al., 2021; Bugueño and de Melo, 2023; Wang et al., 2023). Earliest approaches, such as TextRank (Mihalcea and Tarau, 2004; Hassan et al., 2007) and LexRank (Erkan and Radev, 2004), represented words as nodes and their co-occurrences as edges. However, they lacked deep semantic structure despite a densely connected network (Bugueño and de Melo, 2023).

Other approaches have designed document graphs that integrate both linguistic and semantic knowledge while exploring multiple levels of granularity. Nodes may represent linguistic units—such as morphemes, words, phrases, sentences, or entire documents (Qian et al., 2018; Yao et al., 2019)—or semantic units, including entities, keywords, or events (Zeng et al., 2020; Hua et al., 2023). Correspondingly, edges encode structural or semantic relationships among these units. Some work (e.g., Wang et al. (2023)) further introduce multiple types of nodes and edges to facilitate coexisting diverse forms of information propagation.

Nevertheless, heavily tailored graph representations are not necessarily beneficial. On text classification tasks, simple word-level co-occurrence graphs proved to be sufficient (Castillo et al., 2017). Notably, such simpler structures tend to yield bet-

ter performance on longer documents while being more computationally efficient (Bugueño and de Melo, 2023). This may be because complex or noisy graphs hinder effective learning, even for specialized graph-based learning models. Assuming dense and long-range relations between nodes could benefit a global view, but it is not necessarily optimal for learning. Excessive connectivity could lead to *oversmoothing*, where node representations become indistinguishable after iterative neighborhood aggregation (Zhang et al., 2020; Plenz and Frank, 2024).

Moreover, heuristic-based graph constructions often rely on feature selection, which might not generalize well in cross-domain or cross-task settings. Also, extracting features from documents may rely on external processing steps, e.g., part-of-speech tagging, named entity recognition, and coreference resolution, which can introduce cascading errors throughout the learning process.

2.3 Combining Graph and LMs

Recent work has explored hybrid approaches that combine textual and structural representations. These methods integrate the rich contextual understanding of LMs with the relational reasoning capabilities of graphs to improve performance across various NLP tasks.

ConTextING (Huang et al., 2022) unified pre-trained BERT embeddings with inductive graph neural networks (GNNs) to jointly learn document-level context and fine-grained word interactions via a sub-word graph, highlighting contextual word semantics and graph-based reasoning.

Similarly, Onan (2023) presented a hierarchical graph-based framework by combining linguistic features, domain-specific graph construction, and contextual embeddings. The model integrates multi-level graph learning and attention mechanisms to capture complex structural relationships, and a dynamic fusion layer that combines these with BERT representations.

Plenz and Frank (2024) introduced the Graph Language Model (GLM), which jointly encodes text and graph triplets, enabling unified reasoning over linguistic and structural information while retaining the expressive contextual representations of language models.

2.4 Learned Graph Representations

Despite recent advances, most graph-based representations still depend on heuristic or manually en-

gineered construction methods. Consequently, they may not generalize well across diverse domains nor be able to handle modern document processing challenges, such as capturing long-distance and non-linear dependencies, or managing imbalanced or lengthy document inputs.

To overcome these limitations, [Xu et al. \(2021\)](#) proposed a hybrid approach that trains a Graph Attention Network (GAT) ([Veličković et al., 2017](#)) on passage embeddings in each document and employs contrastive learning to refine document representations in an unsupervised manner. GraphLSS ([Bugueño et al., 2025](#)) proposed automatically constructible heterogeneous graph representations by integrating lexical, structural and semantic information, resulting in a more interpretable and efficient alternative.

Drawing on these ideas, [Bugueño and de Melo \(2025\)](#) proposed a fully data-driven approach that constructs graphs directly from raw text, eliminating the need for handcrafted construction rules and domain dependency. Their method leveraged pre-trained language models and full self-attention mechanisms to model contextual relationships between sentences, enabling the automatic induction of meaningful graph structures. To enhance sparsity and efficiency, they applied statistical filtering to retain only salient relationships, yielding sparse yet informative graphs. Results showed that models trained on these learned attention-induced graphs consistently outperformed heuristic-based counterparts, highlighting both the robustness and adaptability of this approach while reducing manual and domain-specific dependencies.

However, while [Bugueño and de Melo \(2025\)](#) effectively captured global contextual dependencies, their reliance on full attention mechanisms introduces quadratic computational complexity. Moreover, global attention is not always necessary, especially in long documents, as distant sentences may share little semantic relevance. Prior research, such as [Beltagy et al. \(2020\)](#) and [Zaheer et al. \(2020\)](#) showed that local and mid-range context modeling can capture most of the essential information with substantially lower resource demands.

Based on these insights, this work investigates how graph-based representations can more effectively and efficiently exploit localized contextual dependencies while maintaining strong semantic coherence.

3 Method

Overall, our methodology closely follows [Bugueño and de Melo \(2025\)](#)’s procedure. However, we replace the full-attention modules with sliding-window attention (SWA). As implemented in models such as Longformer ([Beltagy et al., 2020](#)), sliding-window attention restricts each sentence’s attention to a local neighborhood. It enhances sensitivity to local and mid-range contextual relationships while substantially improving computational efficiency and robustness.

The window size, therefore, plays a critical role in balancing contextual coverage and noise: smaller windows emphasize local coherence but limit global context, whereas larger windows capture broader dependencies at the risk of introducing irrelevant information and increased computational overhead.

While [Bugueño et al. \(2025\)](#) report optimal performance using a window size of 40%—defined by the number of sentences in each document, and based on sentence similarity—we hypothesize that learned attention weights provide a more effective way to identify task-relevant context. This allows the use of substantially smaller windows without degrading performance. Moreover, the dynamic adjustment to the input size allows consistent handling of documents of varying lengths. Our window-size ablation study in [Section 5.3](#) supports this hypothesis.

Furthermore, this paper explores strategies to obtain high-quality attention weights and incorporates them into graph construction. The key components of this process are: (1) **non-linear transformations** of the attention weights, and (2) **statistical filtering** to enforce sparsity.

Several previous research studies empirically demonstrated that activation functions can modulate raw attention weights, leading to more expressive results and capturing complex relationships between tokens. They could introduce task-specific biases that benefit models in learning more than others ([Sharma et al., 2017](#)) (See [Figure 3](#)).

Similarly, the statistical filtering step helps to prune weak connections and retain the most salient dependencies. [Bugueño and de Melo](#)’s results showed that mean-bound filtering showed optimal results for medium-length document processing, while max-bound filtering is optimal for long document processing.

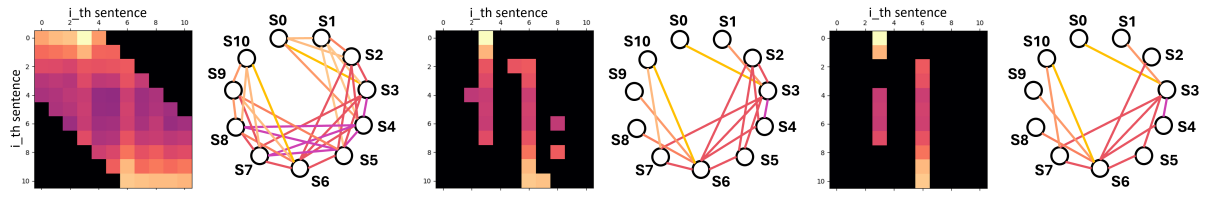


Figure 1: Attention matrix from a random document in the HND dataset paired with graphs constructed according to different statistical filtering: non-filtered (Left), mean-bound filter (Middle), and max-bound filter (Right). Brighter colors illustrate higher values.

3.1 Sliding Window Attention Models

We first encode each document D using a pre-trained Sentence Transformer model, mapping every sentence s_i to its corresponding embedding x_i . Then, the resulting set of embeddings X constitutes the input to the SWA models.

The self-attention layer is implemented as a sliding-window multi-head attention mechanism that restricts attention computation to tokens within the defined window size or a predefined maximum cut-off length. For the non-linear transformation, we evaluate multiple activation functions that have shown strong performance in previous studies (specifically ReLU (Wortsman et al., 2023; Bugueño and de Melo, 2025) and Sigmoid (Rampuram et al., 2024) in addition to the conventional Softmax, to assess their effect on model expressiveness and stability.

To compute scaled dot-product attention weights, we define each activation as follows:

$$\text{Attention}_{softmax} = \text{softmax} \left(\frac{A}{T} \right) \quad (1)$$

$$\text{Attention}_{relu} = \frac{\text{ReLU}(A)}{d} \quad (2)$$

$$\text{Attention}_{sigmoid} = \sigma(A - \log d) \quad (3)$$

where A is the attention logits, T the temperature, and $d = \dim(A_{-1})$ be the size of the last dimension of A , corresponding to the document length measured in sentences.

The default temperature is set to 1. However, since previous literature showed that annealing temperature helped gradually sharpen attention distributions during training (Caron et al., 2021), we also experimented with annealing scheduling, decreasing it by 0.0004 per batch, down to the minimum of 0.1, as seen in Equation 4.

$$T = \max \left(0.1, e^{-\lambda \cdot i} \right) \quad (4)$$

where λ is the annealing rate and i is the global iteration index. Further implementation details on SWA models are provided in Appendix B.

3.2 Graph Construction and Filtering

A document graph is defined as $G = (V, E)$, where V is the set of sentence nodes and E is the set of edges. Nodes v_i and v_j are connected by an undirected weighted edge α_{ij} if the attention weight W_{ij} exceeds a predefined threshold τ after being adjusted by the tolerance degree δ .

We adopt the two thresholds—mean-bound and max-bound—from the previous work (Bugueño and de Melo, 2025). Mean-bound filter sets a threshold slightly above a sentence’s average attention score to retain more relevant dependencies. On the other hand, max-bound sets a threshold slightly below a sentence’s maximum attention score to retain only the strongest connections. Each threshold is calculated row-wise, so that each node is connected to at least one node. We also merge nodes with identical embeddings into a single node to reduce redundancy. However, after all steps, if a node is only connected to itself, we divide the weight α_{ii} by 2, then allocate the weight to $\alpha_{i-1,i}$ and $\alpha_{i,i+1}$.

Figure 1 illustrates the graph construction process using each type of statistical filtering.

4 Experiments

We hypothesize that an effective graph-based representation should encode sufficient task-relevant information to support downstream NLP tasks. To evaluate this, we focus primarily on document classification, a common yet challenging task for assessing a model’s ability to capture document-level semantics and structural information.

We examine our approach along three key aspects: (i) classification performance, (ii) graph structure, and (iii) choice of window size. Specifically, we compare graph variants generated by SWA models with different nonlinear activation

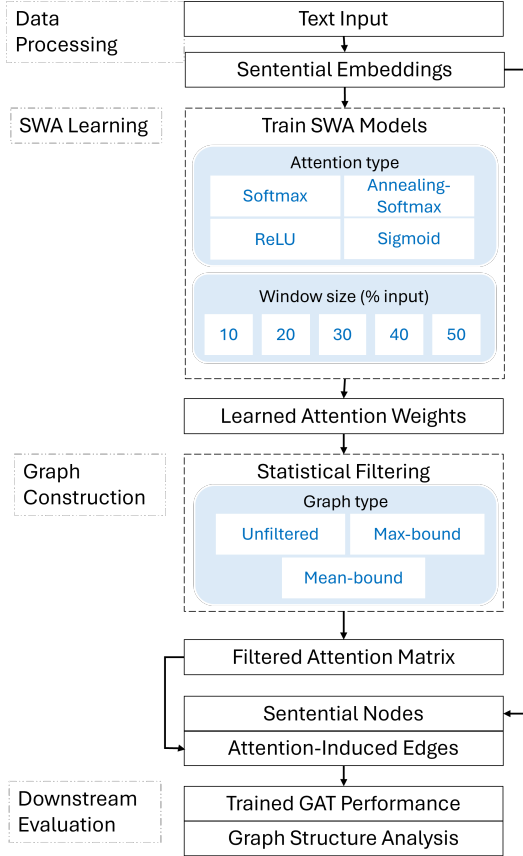


Figure 2: Overview of our experiment pipeline. The experimental components are illustrated in blue.

functions, as well as graphs constructed with and without statistical filtering. We further analyze the resulting graph structures with a focus on computational efficiency. To assess sensitivity to contextual scope, we conduct a window-size ablation on one dataset, varying the window from 10% to 50% of the document length, measured in sentences.

In addition, we explore (iv) an extension to extractive document summarization to examine generality and task-specific limitations.

Across tasks, we train Graph Attention Network (GAT) models on our constructed graphs and evaluate performance using accuracy and F1 score, which respectively capture overall and class-level performance, particularly in class-imbalanced settings. Implementation details of the GAT models are provided in Appendix B. Figure 2 illustrates the proposed framework and the experiment pipeline.

4.1 Datasets

Three publicly available classification datasets are employed in our main experiments. To ensure direct comparability, we reuse all three document classification datasets from Bugueño and de Melo

Dataset	K	Ratio	Length	Samples
BBC	5	4:5	19	2,225
HND	2	1:2	21	1,270
AX	11	1:2	539	33,388

Table 1: Datasets summary. *Ratio* denotes the class imbalance (major/minor), and *Length* reports the average number of sentences per document.

(2025). A summary of the datasets is provided in Table 1, with further details in Appendix A.

- **BBC News (BBC)** (Greene and Cunningham, 2006) comprises 2,225 medium-length news articles categorized into five relatively balanced topics.
- **Hyperpartisan News Detection (HND)** (Kiesel et al., 2019) contains 1,270 news articles with imbalance labels of hyperpartisan or non-hyperpartisan.
- **arXiv classification (AX)²** (He et al., 2019) consists of 33,388 long scientific arXiv papers across 11 classes with slight imbalance.

Baselines We use the heuristic baselines studied by Bugueño and de Melo (2025), including sentence-order, fixed-size window co-occurrence, mean-bound semantic similarity, and max-bound semantic similarity, as well as their reported results.

5 Results

Section 5.1 and Section 5.2 present the results on document classification performance and graph efficiency, respectively, including direct comparisons with prior work (Bugueño and de Melo, 2025). Section 5.3 details a window size ablation study on the HND dataset and its impact on model performance. Furthermore, Section 5.4 presents the results of exploratory experiments on document extractive summarization. Additional results and corresponding t-test analyses are provided in Appendix C.

5.1 Classification Performance

Table 2 presents a comparison of our *best* performing models against two categories of baselines: (1) baselines from previous work, namely learned graphs induced from full-attention models with statistical filtering, and (2) multi-head SWA models,

²Due to the size of the dataset and resource constraints, we only experiment with max-bound graphs with Softmax attention-as the standard variant, and ReLU attention, to enable comparison with previous work.

Dataset	Graph Type	Scheme	Acc	F1	V	E	Degree	Disk	Variant
BBC	heuristic	order	99.7	99.7	19.3	36.6	1.9	74 M	2-64
	heuristic	window	99.8	99.8	19.3	71.2	3.7	76 M	2-64
	heuristic	mean semantic	99.4	99.3	19.3	159.7	5.4	84 M	2-64
	heuristic	max semantic	99.7	99.7	19.3	36.7	1.9	74 M	2-64
	full-attention	mean-bound (2025)	99.9	99.9	19.3	245.8	9.5	90 M	ReLU-2-64
	full-attention	max-bound (2025)	99.6	99.6	19.3	66.3	3.4	77 M	ReLU-2-64
	non-graph	SWA	94.6	94.3	–	–	–	–	ReLU-1-128
	SW-attention	unfiltered	100.0	100.0	19.3	537.4	27.9	113 M	various models
	SW-attention	mean-bound	100.0	99.9	19.3	152.0	7.9	84 M	Sigmoid-2-64
SW-attention	max-bound	99.9	99.9	19.3	67.0	3.5	77 M	ReLU-2-256	
HND	heuristic	order	92.6	92.6	19.5	37.0	1.8	43 M	3-64
	heuristic	window	92.1	92.1	19.5	72.0	3.4	44 M	3-64
	heuristic	mean semantic	91.2	91.1	19.5	254.8	6.0	53 M	3-64
	heuristic	max semantic	92.8	92.8	19.5	36.9	1.8	43 M	3-64
	full-attention	mean-bound (2025)	95.0	94.9	19.5	329.6	8.9	56 M	ReLU-3-64
	full-attention	max-bound (2025)	92.6	92.6	19.5	57.4	2.8	44 M	ReLU-3-64
	non-graph	SWA	76.2	76.1	–	–	–	–	Sigmoid-1-128
	SW-attention	unfiltered	95.0	95.0	19.5	768.2	39.0	72 M	Softmax-2-128
	SW-attention	mean-bound	94.8	94.7	19.5	183.4	9.3	47 M	Sigmoid-2-128
SW-attention	max-bound	95.5	95.5	19.5	56.4	2.9	42 M	Sigmoid-2-256	
AX	heuristic	order	87.3	86.7	510.3	1035.0	2.0	25 GB	3-64
	heuristic	window	87.9	87.4	510.3	1068.3	4.0	26 GB	3-64
	heuristic	max semantic	87.8	87.4	510.3	1241.9	2.3	26 GB	3-64
	full-attention	max-bound (2025)	91.9	91.7	510.3	1092.2	2.2	25 GB	ReLU-3-64
	non-graph	SWA	84.6	84.2	–	–	–	–	ReLU-1-128
	SW-attention	max-bound	92.2	91.9	510.3	1281.5	2.5	26 GB	Softmax-3-64

Table 2: Accuracy, F1 score, and average graph structural statistics on each dataset, compared to Bugueño and de Melo (2025). Variants consist of attention-type (if applicable), and the number of GAT layers and hidden units.

whose attention weights serve as the basis for constructing our attention-induced graphs.

The locally aware attention-induced graphs outperform the previously best full-attention graphs based on mean-bound ReLU attention (Bugueño and de Melo, 2025) across all datasets. While prior work emphasized the importance of global context, our results demonstrate that focusing on local and mid-range semantic dependencies is effective.

On the medium-length BBC and HND datasets, mean-bound filtering yields only marginal gains, likely because this strategy is already near-optimal, with no significant difference from max-bound filtering. In some cases, non-filtered graphs perform best, achieving near-perfect accuracy and F1 scores on BBC and consistent improvements of approximately 0.5-3 points on HND. Performance difference among attention types alone remains marginal, although some combinations of attention type and statistical filters show significant gain (see Table 9, Table 10, Table 11, Table 12, and Table 13 in Appendix C).

Consistent with prior work, max-bound filtering is more effective for longer documents, suggesting that salient dependencies are best captured locally. Applying this filter to sliding-window attention weights proves more expressive than applying it to full-attention weights. Conversely, the weaker

performance of mean-bound graphs indicates that certain informative dependencies may still benefit from global context, as previously observed in full attention-based graph constructions.

Graphs constructed without statistical filtering yield competitive performance, albeit being denser and potentially noisier, as they retain all soft dependencies. This indicates that GAT models trained on such graphs may implicitly suppress irrelevant connections or exploit expressive yet non-salient dependencies that are subsequently removed by our statistical filters; for instance, salient dependencies that are eliminated under row-wise thresholding but would be preserved under a global criterion.

At the current scale and chosen window size, the increased graph density does not yet translate into prohibitive inefficiencies, although non-filtered graphs incur markedly higher memory and computational costs. Anecdotally, training and inference times remain comparable between filtered and non-filtered graphs³. Overall, these results expose a clear trade-off between computational cost and performance: non-filtered sliding-window attention graphs offer statistically significant gains ($p <$

³Since training and inference times could vary due to the influence of hardware, we do not officially report them here. Still, the information is logged and reported in the GNN_Results folder in our public repository.

0.05) at the cost of increased resource usage.

5.2 Graph Structural Analysis

We compare the graph structures induced by sliding-window attention models to Bugueño and de Melo (2025)’s full attention-induced graphs. Learned sliding-window attentions with statistical filtering produce comparatively sparse graphs that retain local-contextual key links while reducing resource usage and improving model performance.

Consistent with the previous work, the proposed statistical filtering—applied on top of learned attention matrices—consistently results in graphs with improved structural coherence, higher resource efficiency, and better information preservation compared to heuristic constructions. As a result, the induced graphs achieve superior classification performance. Moreover, the sparsity introduced by statistical filtering not only improves efficiency but also supports better generalization across tasks.

The number of edges in our graphs after applying mean-bound filtering is about 40% fewer edges than the full-attention graphs induced with the same filter. These graphs are smaller on disk and scale better, both computationally and memory-wise. Training remains efficient, with complexity growing linearly despite input length (Beltagy et al., 2020). Meanwhile, the average number of edges and disk size in our max-bound graphs may be negligibly higher than those in full-attention graphs with the same filter—indicating denser yet more evenly distributed attention across nodes—while exhibiting similar sparsity patterns. Nevertheless, these results suggest that denser local neighborhoods can provide rich contextual information.

Despite their compactness, these graphs remain informative, thus sufficient for models as shallow as one-layer GATs to learn meaningful graph-based document representations.

5.3 Window Size Ablation

We perform an ablation study to assess the effect of window size in our pipeline. Notably, given that the performance of our model approaches the optimal on the BBC dataset and that the AX dataset is exceptionally large, we restrict this analysis to the HND dataset. Table 3 reports the results for both sliding-window attention (SWA) models and GAT models.

While SWA models exhibit only marginal sensitivity to the choice of window size, GATs trained with a 30% window consistently outperform al-

Window size	SWA		GAT	
	Acc	F1	Acc	F1
10	78.9	73.1	92.1	92.1
20	76.4	74.6	92.0	92.0
30	76.6	73	92.7	92.6
40	77.0	73.6	91.2	91.1
50	73.8	74.9	91.9	91.9
100	75.1	75	93.0	92.3

Table 3: Accuracy and F1 score on the HND dataset. As in the main results table, results are averaged over 5 independent runs. GAT results report the average of 3 graph types: unfiltered, mean-bound and max-bound. The full-attention setting (100% window) and its respective GAT results serve as a baseline.

ternative settings, supporting our hypothesis (see Table 14). Although full attention-induced graphs yield the best GAT results, the gain is marginal. In contrast, a 40% window consistently degrades performance across all GAT configurations.

A fine-grained analysis reveals two notable trends: (i) smaller windows (10–30%) are more effective when applied to unfiltered graphs, whereas (ii) larger windows (e.g., 50%) yield improved performance when combined with statistical filtering. These observations suggest that narrower contextual scopes allow models to better exploit dense local structure and sentence-order information, while broader semantic contexts benefit from sparsification. On the other hand, when dense graphs are paired with wide contextual windows, competing signals may hinder effective learning.

For long-document settings such as arXiv, reducing the window size yields only marginal performance differences. Nevertheless, replacing prohibitively expensive full attention-induced graph construction with sliding-window variants remains advantageous due to improved scalability and reduced computational cost. More generally, locally relevant context does not scale linearly with document length, suggesting that future work should further investigate how the appropriate context scope should adapt as documents grow.

5.4 Adaptation to Document Summarization

To further validate our graph construction approach, we conduct an exploratory experiment on document extractive summarization, which also requires an understanding of both document semantics and structure.

We conduct experiments on the GovReport (GR) dataset (Huang et al., 2021)—a dataset that contains long U.S. Government reports—, as well as

Graph Type	Scheme	Acc	F1	F1 per class		Variant
				summary	non-summary	
heuristic	order	68.1	53.4	79.5	27.4	2-256
heuristic	fixed window	68.9	47.2	79.7	28.6	2-256
non-graph	SWA	75.3	53.4	85.4	21.4	ReLU-1-128
SW-attention	max-bound	72.0	56.9	82.4	31.5	Softmax-2-256
SW-attention	mean-bound	61.9	48.2	74.8	21.7	Annealing-3-128

Table 4: Performance comparison on the **GR** summarization task. F1 scores are reported at the macro and class levels. Variant consists of attention-type (if applicable), number of GAT layers, and number of hidden nodes.

two heuristic baselines adopted from Bugueño and de Melo (2025): sentence-order graphs (*order*) and fixed-size co-occurrence window graphs with window size 2 (*fixed window*). We frame summarization as a sentence-level classification task. Specifically, the model predicts whether each sentence is summary-worthy (class 1) or not (class 0), and the selected sentences are then compared against oracle summaries (Liu and Lapata, 2019), as described in Section A.2.

Due to the high computational demands of training on unfiltered graphs, we exclusively train GAT models using filtered graphs, i.e., mean-bound and max-bound. This further underscores the importance of statistical filtering. Additionally, the two-tailed t-test analysis (Table 15) once again confirms that sparse semantic dependencies obtained from max-bound filtering benefit longer document processing.

In contrast to document classification, the summarization results do not show consistent or significant gains from data-driven attention graphs compared to baselines (see Table 16). When averaged across all experimental settings, results suggest that incorporating learned semantic dependencies provides limited overall advantage over pre-defined baselines. Nevertheless, while performance on the minority (summary-worthy) class remains competitive, GAT models often obtain higher overall F1 scores due to improved performance on the majority non-summary class, indicating slightly increased One contributing factor may be the strong effectiveness of order-based connectivity, which captures key signals for extractive summarization, such as sentence position and local neighborhood structure.

However, an analysis of summary sentence position distributions does not provide conclusive evidence that positional information alone accounts for the observed performance trends (see Section D.1). A further limitation arises from the evaluation protocol: performance is measured exclu-

sively against oracle summaries optimized for lexical overlap with human-written references. This formulation may favor keyword-dense sentences over semantically coherent or discourse-relevant content, potentially underestimating the benefits of graph-based semantic modeling. This misalignment is partially supported by our ROUGE and BERTScore analyses (see Section D.3).

Finally, the use of a strongly weighted class loss may bias models toward over-predicting summary-worthy sentences, which can inflate recall at the expense of precision, as shown in Section D.2.

Overall, these findings suggest that the current task formulation and evaluation protocols for extractive summarization place weaker demands on semantic graph structure than document classification, highlighting the limitations of our approach as well as the promising directions for future research on automatic graph generation for summarization.

6 Conclusion

In the current work, we present yet another data-driven approach to build graph-based document representations by utilizing dynamic sliding-window attention models to automatically capture the local and mid-range contextual relationships between sentences. We validate our approach by training GAT models on the graphs constructed with learned attention weights on two common NLP tasks. The results and following analyses demonstrate that even with shallow attention models, our strategy preserves structurally expressive information and highlights semantically salient contextual dependencies in the document; in the meantime, it also optimizes computational resources. This promising outcome opens the door to potential future research on developing graph strategies to induce high-quality localized contexts that can be automatically learned, such as attentions, as well as filtering methods.

Limitations

While our experiments demonstrate the effectiveness of the proposed approach, several aspects warrant further exploration. First, the current evaluation is limited to English-language datasets, primarily within the news domain and of medium to medium-long document length. Extending the analysis to additional languages and domains would provide a more comprehensive assessment of generalization. Second, for the summarization task, evaluation was conducted against oracle summaries only, without direct comparison to human-written gold summaries or qualitative human assessments. Adapting the approach to other downstream tasks and a deeper error analysis could also yield valuable insights into model behavior. Nonetheless, the observed results highlight the promise of our method and motivate future research toward broader applicability and more extensive evaluation.

Acknowledgments

We sincerely thank the EACL 2026 Student Research Workshop (SRW) reviewers for their constructive feedback and insightful comments. We are also grateful to the EACL SRW organizing committee for creating a supportive and engaging environment for early-stage research and scholarly exchange.

References

- Iz Beltagy, Matthew E Peters, and Arman Cohan. 2020. Longformer: The long-document transformer. *arXiv preprint arXiv:2004.05150*.
- Margarita Bugueño, Hazem Abou Hamdan, and Gerard De Melo. 2025. Graphlss: Integrating lexical, structural, and semantic features for long document extractive summarization. In *Proceedings of the 2025 Conference of the Nations of the Americas Chapter of the Association for Computational Linguistics: Human Language Technologies (Volume 2: Short Papers)*, pages 797–804.
- Margarita Bugueño and Gerard de Melo. 2023. Connecting the dots: What graph-based text representations work best for text classification using graph neural networks? *arXiv preprint arXiv:2305.14578*.
- Margarita Bugueño and Gerard de Melo. 2025. [Rethinking graph-based document classification: Learning data-driven structures beyond heuristic approaches](#). Preprint, arXiv:2508.00864.
- Mathilde Caron, Hugo Touvron, Ishan Misra, Hervé Jégou, Julien Mairal, Piotr Bojanowski, and Armand Joulin. 2021. Emerging properties in self-supervised vision transformers. In *Proceedings of the IEEE/CVF international conference on computer vision*, pages 9650–9660.
- Esteban Castillo, Ofelia Cervantes, and Darnes Vilarino. 2017. Text analysis using different graph-based representations. *Computación y Sistemas*, 21(4):581–599.
- Günes Erkan and Dragomir R Radev. 2004. Lexrank: Graph-based lexical centrality as salience in text summarization. *Journal of artificial intelligence research*, 22:457–479.
- Derek Greene and Pádraig Cunningham. 2006. Practical solutions to the problem of diagonal dominance in kernel document clustering. In *Proceedings of the 23rd international conference on Machine learning*, pages 377–384.
- Samer Hassan, Rada Mihalcea, and Carmen Banea. 2007. Random walk term weighting for improved text classification. *International Journal of Semantic Computing*, 1(04):421–439.
- Jun He, Liqun Wang, Liu Liu, Jiao Feng, and Hao Wu. 2019. Long document classification from local word glimpses via recurrent attention learning. *IEEE Access*, 7:40707–40718.
- Yilun Hua, Zhaoyuan Deng, and Kathleen McKeown. 2023. Improving long dialogue summarization with semantic graph representation. In *Findings of the Association for Computational Linguistics: ACL 2023*, pages 13851–13883.
- Luyang Huang, Shuyang Cao, Nikolaus Parulian, Heng Ji, and Lu Wang. 2021. Efficient attentions for long document summarization. *arXiv preprint arXiv:2104.02112*.
- Yen-Hao Huang, Yi-Hsin Chen, and Yi-Shin Chen. 2022. Contexting: granting document-wise contextual embeddings to graph neural networks for inductive text classification. In *Proceedings of the 29th international conference on computational linguistics*, pages 1163–1168.
- G Thomas Hudson and Noura Al Moubayed. 2022. Muld: The multitask long document benchmark. *arXiv preprint arXiv:2202.07362*.
- Johannes Kiesel, Maria Mestre, Rishabh Shukla, Emmanuel Vincent, Payam Adineh, David Corney, Benno Stein, and Martin Potthast. 2019. Semeval-2019 task 4: Hyperpartisan news detection. In *Proceedings of the 13th International Workshop on Semantic Evaluation*, pages 829–839.
- Diederik P Kingma and Jimmy Ba. 2014. Adam: A method for stochastic optimization. *arXiv preprint arXiv:1412.6980*.

- Olga Kovaleva, Alexey Romanov, Anna Rogers, and Anna Rumshisky. 2019. Revealing the dark secrets of bert. *arXiv preprint arXiv:1908.08593*.
- Chin-Yew Lin. 2004. Rouge: A package for automatic evaluation of summaries. In *Text summarization branches out*, pages 74–81.
- Yang Liu and Mirella Lapata. 2019. Text summarization with pretrained encoders. *arXiv preprint arXiv:1908.08345*.
- Congbo Ma, Wei Emma Zhang, Mingyu Guo, Hu Wang, and Quan Z Sheng. 2022. Multi-document summarization via deep learning techniques: A survey. *ACM Computing Surveys*, 55(5):1–37.
- Rada Mihalcea and Paul Tarau. 2004. Textrank: Bringing order into text. In *Proceedings of the 2004 conference on empirical methods in natural language processing*, pages 404–411.
- Aytuğ Onan. 2023. Hierarchical graph-based text classification framework with contextual node embedding and bert-based dynamic fusion. *Journal of king saud university-computer and information sciences*, 35(7):101610.
- Moritz Plenz and Anette Frank. 2024. Graph language models. *arXiv preprint arXiv:2401.07105*.
- Yujie Qian, Enrico Santus, Zhijing Jin, Jiang Guo, and Regina Barzilay. 2018. Graphie: A graph-based framework for information extraction. *arXiv preprint arXiv:1810.13083*.
- Jason Ramapuram, Federico Danieli, Eeshan Dhekane, Floris Weers, Dan Busbridge, Pierre Ablin, Tatiana Likhomanenko, Jagrit Digani, Zijin Gu, Amitis Shidani, and 1 others. 2024. Theory, analysis, and best practices for sigmoid self-attention. *arXiv preprint arXiv:2409.04431*.
- Sagar Sharma, Simone Sharma, and Anidhya Athaiya. 2017. Activation functions in neural networks. *Towards Data Sci*, 6(12):310–316.
- Aaron Van Den Oord, Sander Dieleman, Heiga Zen, Karen Simonyan, Oriol Vinyals, Alex Graves, Nal Kalchbrenner, Andrew Senior, Koray Kavukcuoglu, and 1 others. 2016. Wavenet: A generative model for raw audio. *arXiv preprint arXiv:1609.03499*, 12:1.
- Petar Veličković, Guillem Cucurull, Arantxa Casanova, Adriana Romero, Pietro Lio, and Yoshua Bengio. 2017. Graph attention networks. *arXiv preprint arXiv:1710.10903*.
- Dongsheng Wang, Zhiqiang Ma, Armineh Nourbakhsh, Kang Gu, and Sameena Shah. 2023. Docgraphlm: Documental graph language model for information extraction. In *Proceedings of the 46th International ACM SIGIR Conference on Research and Development in Information Retrieval*, pages 1944–1948.
- Kunze Wang, Yihao Ding, and Soyeon Caren Han. 2024. Graph neural networks for text classification: A survey. *Artificial intelligence review*, 57(8):190.
- A Waswani, N Shazeer, N Parmar, J Uszkoreit, L Jones, A Gomez, L Kaiser, and I Polosukhin. 2017. Attention is all you need. In *NIPS*.
- Mitchell Wortsman, Jaehoon Lee, Justin Gilmer, and Simon Kornblith. 2023. Replacing softmax with relu in vision transformers. *arXiv preprint arXiv:2309.08586*.
- Peng Xu, Xinchu Chen, Xiaofei Ma, Zhiheng Huang, and Bing Xiang. 2021. Contrastive document representation learning with graph attention networks. *arXiv preprint arXiv:2110.10778*.
- Liang Yao, Chengsheng Mao, and Yuan Luo. 2019. Graph convolutional networks for text classification. In *Proceedings of the AAAI conference on artificial intelligence*, volume 33, pages 7370–7377.
- Manzil Zaheer, Guru Guruganesh, Kumar Avinava Dubey, Joshua Ainslie, Chris Alberti, Santiago Ontanon, Philip Pham, Anirudh Ravula, Qifan Wang, Li Yang, and 1 others. 2020. Big bird: Transformers for longer sequences. *Advances in neural information processing systems*, 33:17283–17297.
- Shuang Zeng, Runxin Xu, Baobao Chang, and Lei Li. 2020. Double graph based reasoning for document-level relation extraction. *arXiv preprint arXiv:2009.13752*.
- Tianyi Zhang, Varsha Kishore, Felix Wu, Kilian Q Weinberger, and Yoav Artzi. 2019. Bertscore: Evaluating text generation with bert. *arXiv preprint arXiv:1904.09675*.
- Yufeng Zhang, Xueli Yu, Zeyu Cui, Shu Wu, Zhongzhen Wen, and Liang Wang. 2020. Every document owns its structure: Inductive text classification via graph neural networks. *arXiv preprint arXiv:2004.13826*.

A Datasets

A.1 Document Classification Datasets

BBC News (Greene and Cunningham, 2006) is a collection of 2,225 news articles from the BBC News website. The articles are considered medium-length and are labeled according to the five topics: business, entertainment, politics, sport, and technology. The labels are relatively balanced.

Hyperpartisan News Detection (HND) (Kiesel et al., 2019) is a collection of 645 news articles, with binary labels as hyperpartisan or non-hyperpartisan, categorizing if a news article ignores or attacks the opposing views blindly. The dataset is relatively small and imbalanced. Moreover, the dataset contains some relatively long documents,

namely, over 5% of the documents contain more than 50 sentences.

Extended **arXiv document classification (AX)** (He et al., 2019) consisting of 33,388 papers across 11 subject categories in Mathematics and Computer Science. The label expands a previously released 4-class version to a more diverse and challenging multi-class setting through a weakly supervised method. Each document contains at least 1,000 words and is truncated within 10,000 words.

A.2 Document Summarization Dataset

GovReport (hence, GR) (Huang et al., 2021) is a collection of 19,466 reports from the U.S. Government Accountability Office, covering a wide range of national policy issues. The gold summaries were human-written and abstractive.

To adapt to the current extractive summarization task, oracle summaries (Liu and Lapata, 2019) have been prepared by including sentences that maximize the Rouge-1 score (Lin, 2004); in other words, the overlap between selected sentences and the original summaries.

We then frame the summarization task as a sentence classification task, where each sentence in a document is individually labeled as either to be included in the summary or not. While a report contains an average of 300 sentences, approximately 10 are included in the summary. Therefore, the corresponding extractive sentence labels are extremely unbalanced.

B Implementation Details

The project is implemented mainly in PyTorch framework. PyTorch Geometric is used to construct graph datasets and train GAT models.

All experiments were run on NVIDIA GeForce RTX 3090, except the window ablation study were run on Google Colab T4.

B.1 Setup

Learned attention weights used to construct attention-induced graphs are extracted from multi-head SWA models. These graphs are then used to train Graph Attention Network (GAT) models in order to evaluate the efficiency of our approach. We deliberately employ a simple SWA architecture to demonstrate the effectiveness of the data-driven method at a foundational level, serving as a baseline for more advanced extensions. In parallel, we evaluate multiple GAT architectures to assess the

robustness of the proposed graph construction strategy across different model configurations.

Nonetheless, both types of models, the learning rate is 0.001. The batch size is set to 32. Dropout is applied to each fully connected layer with a rate of 0.2. Class weights are applied to the cross-entropy loss function to reduce bias toward the majority classes.

B.2 Multi-Head SWA Models

Sentence embeddings are obtained using a frozen pretrained model: SentenceTransformer (paraphrase-MiniLM-L6-v2)⁴ with its 384 embedding dimensions. A multi-head self-attention (MHA) model is comprised of the following trainable layers: two fully connected layers of 128 hidden nodes with Xavier-uniform initialization, a sliding-window attention layer, and a non-linear layer. We employ 4 self-attention heads, and compute attention using scaled dot-product; then, we concatenate and pass it through the output projection layer.

The model can be trained up to 20 epochs using Adam optimization (Kingma and Ba, 2014); however, if the macro-averaged F1 score on the validation split does not improve by at least 0.001 during the following five epochs, the training is interrupted.

For each setting, we initialize and train five models independently and evaluate them against the F1 score on the validation set. Later, the learned attention weights from the MHA models with consistently higher F1 scores are used to construct graphs.

B.3 Graph Attention Models

We experiment with the number of GAT layers and hidden nodes, from {1, 2, 3} and {64, 128, 256} respectively. The models can be trained up to 50 epochs, but they are interrupted if the F1 score on the validation set does not improve by at least 0.001 in the five consecutive epochs. For each GAT setting, we obtain results from five independent runs and average them.

C Detailed GAT Results

Due to practicality and space constraints, we only report average GAT results with the two studied components in Table 5 (BBC), Table 6 (HND), Table 7 (AX) and Table 8 (GR).

⁴<https://huggingface.co/sentence-transformers/paraphrase-MiniLM-L6-v2>

However, our study explores various combinations of non-linear activation functions, hidden layers, hidden nodes, and statistical filters, resulting in 108 configurations for the BBC dataset and 72 each for the HND and GR datasets, with 5 independent runs per configuration⁵.

C.1 Independent T-Test Analyses

We conduct independent t-test analyses determining whether the result of each of the interested components, i.e., activation functions, statistical filters, and their combinations, is statistically significant from the baselines and from other variants. Likewise, we only present the analyses that are significant.

Table 9 (top) shows a general trend that unfiltered graphs elicit significantly better results. As discussed earlier, Table 10 and Table 11 indicate that several variants of annealing-attention graphs and sigmoid-attention graphs bring out better performance on the BBC dataset.

In both analyses observed in Table 12 and Table 13, unfiltered graphs generated from conventional Softmax induce significantly better performance on the HND dataset.

Table 14 shows that window size of 30% elicited significantly better performance. While the size of 40% is significant, it reveals inadequate performance compared to the other size.

None of the t-test results for AX is present, as none is found to be significant.

As for GR dataset, Table 9 (bottom) displays that max-bound is significantly a better filter than mean-bound. Most of the significant difference in Table 15 seems to be inherited from the filtering, and not the combination themselves. In Table 16, we compare our results to the order-based heuristic baselines. However, our graphs do not show a significant boost. On the other hand, our ReLU-SWA graphs with mean-bound filter are significantly worse than heuristic graphs.

In all datasets, the types of activation functions never solely show greater performance than the others. However, by looking at the attention matrices (see Figure 3), we can observe how different non-linear transformations may map contextual dependencies.

Dataset	Filter	None	Max	Mean
BBC	None		0.0792	0.0005
	Max	0.0417		0.003
GR	Mean	0.0001	0.15	
	Max			0.0002
	Mean		< 0.0001	

Table 9: T-test results of GAT models’ performance when training on graphs with different statistic filters on two datasets. The bottom and left side measure the accuracy scores, and the top and right side measure the F1 scores on the test set. Statistical significance is highlighted in **bold**.

D Investigation into Extractive Summarization

The predicted summaries for this investigation are produced using the prediction on the test split from the best model in the experiments, ReLU-SWA weights with max-bound filter.

D.1 Summary Sentence Distribution

Assuming GAT models might benefit from the order of the sentences, we checked if there is a tendency that a summary sentence is likely to appear in any relative position. The findings indicate only a weak positional trend that earlier sentences are somewhat more likely to appear in summaries, whereas later ones are less likely. Beyond this, however, we did not observe any systematic positional bias in either the oracle or the predicted summaries. Summary sentences are shown to spread throughout the entire document (see Figure 5).

Although we could not prove that there is a relative order of summary sentences, we also could not rule out the possibility that heuristic graphs preserve certain information related to sentence order that is overlooked by attention-based graphs.

D.2 Ratio of Summary Sentences

The result of this investigation exhibits the tendency of the GAT model to over-predict sentences to be a part of summaries. While an oracle summary includes an average of 6% of sentences in a document, the model predicts that roughly 20% of sentences should be included (see Section D.1). It also shows exponential trends to include more sentences as a part of the summary when a document is longer (see Figure 6).

A strong bias towards including sentences in the summary may result from a weighted loss function, model parameter settings, or even the ordering of the training samples.

⁵All detailed results are kept in the GNN_Results subfolder in our GitHub repository.

Attention	Filter	Acc	Acc (std)	F1	F1 (std)	F1 per class				
						sport	entertain	business	tech	politics
Anneal	none	99.80	0.16	99.80	0.16	99.98	99.91	99.63	99.87	99.56
	max	99.29	0.40	99.28	0.41	99.80	99.40	98.98	99.34	98.83
	mean	99.34	0.32	99.32	0.34	99.76	99.36	99.12	99.39	98.97
Softmax	none	99.67	0.20	99.62	0.23	99.96	99.80	99.50	99.72	99.36
	max	99.44	0.34	99.42	0.39	99.81	99.52	99.14	99.62	99.08
	mean	99.37	0.33	99.35	0.35	99.81	95.86	99.12	99.45	98.95
ReLU	none	99.71	0.31	99.70	0.34	99.91	88.63	99.63	99.68	99.51
	max	99.46	0.30	99.42	0.33	99.79	99.48	99.30	99.54	99.09
	mean	99.39	0.18	99.35	0.20	99.86	99.42	99.16	99.49	98.82
Sigmoid	none	99.71	0.21	99.70	0.22	99.88	99.84	99.61	99.83	99.34
	max	99.34	0.24	99.30	0.28	99.84	99.41	99.09	99.51	98.67
	mean	99.63	0.22	99.61	0.21	99.89	99.71	99.51	99.68	99.27

Table 5: GAT results of **BBC** dataset, with each attention type and filters, averaged across 5 independent runs, numbers of layers ($\{1, 2, 3\}$) and hidden nodes ($\{64, 128, 256\}$).

Attention	Filter	Acc	Acc (std)	F1	F1 (std)	F1 per class	
						non-hyperpartisan	hyperpartisan
Anneal	none	91.38	1.83	91.37	1.84	90.93	91.78
	max	92.37	2.63	92.32	2.66	91.92	92.68
	mean	92.22	1.76	92.22	1.76	91.77	92.62
Softmax	none	94.30	0.64	94.30	0.64	94.12	94.45
	max	91.92	2.24	91.88	2.28	91.45	92.27
	mean	91.77	1.85	91.73	1.89	91.23	92.23
ReLU	none	92.00	2.15	91.95	2.16	91.58	92.32
	max	91.75	1.63	91.70	1.66	91.22	92.18
	mean	92.37	2.19	92.35	2.20	91.97	92.77
Sigmoid	none	91.82	1.90	91.82	1.90	91.45	92.18
	max	92.15	2.50	92.07	2.52	91.75	92.52
	mean	92.33	2.57	92.27	2.60	91.93	92.62

Table 6: GAT results of **HND** dataset, with each attention type and filters, averaged across 5 independent runs, numbers of layers ($\{1, 2, 3\}$) and hidden nodes ($\{128, 256\}$).

Attention	Filter	Acc	Acc (std)	F1	F1 (std)	F1 per class										
						0	1	2	3	4	5	6	7	8	9	10
Softmax	max	0.908	0.013	0.906	0.013	0.970	0.857	0.764	0.936	0.978	0.910	0.940	0.902	0.930	0.828	0.938
ReLU	max	0.905	0.011	0.901	0.011	0.976	0.894	0.733	0.924	0.977	0.906	0.925	0.912	0.926	0.824	0.923

Table 7: GAT results of **AX** dataset, with each attention type and filters, averaged across 5 independent runs, numbers of layers ($\{1, 2, 3\}$) and hidden nodes ($\{64, 128, 256\}$). The name of the document classes are: Artificial Intelligence, Computational Engineering, Computer Vision, Data Structures, Information Theory, Neural and Evolutionary, Programming Languages, Systems and Control, Commutative Algebra, Group Theory, and Statistic Theory.

Attention	Filter	Acc	Acc (std)	F1	F1 (std)	F1 per class	
						summary	non-summary
Anneal	max	60.70	4.60	48.07	3.60	73.58	22.57
	mean	58.47	2.52	46.03	1.51	71.84	20.24
Softmax	max	61.86	5.01	48.82	3.93	74.54	21.02
	mean	56.77	1.35	45.01	0.81	70.37	19.64
ReLU	max	62.12	5.24	48.97	4.12	74.73	23.19
	mean	57.50	2.23	45.54	1.49	71.30	20.08
Sigmoid	max	60.02	4.57	47.61	3.38	72.97	20.41
	mean	57.17	1.86	40.53	13.49	70.69	17.76

Table 8: GAT results of **GR** dataset, with each attention type and filters, averaged across 5 independent runs, numbers of layers ($\{1, 2, 3\}$) and hidden nodes ($\{64, 128, 256\}$).

Variant	Ann-0	Ann-x	Ann-m	Sft-0	Sft-x	Sft-m	R-0	R-x	R-m	Sgm-0	Sgm-x	Sgm-m
Ann-0		0.002	0.001	0.077	0.015	0.023	0.434	0.007	0.002	0.290	0.000	0.050
Ann-x	0.0024		0.8039	0.0421	0.4505	0.2788	0.0291	0.4178	0.1790	0.0147	0.8939	0.045
Ann-m	0.0016	0.3234		0.0437	0.5674	0.3514	0.0309	0.5328	0.2195	0.0130	0.8810	0.046
Sft-0	0.1362	0.0210	0.0220		0.2026	0.3175	0.5787	0.1548	0.2083	0.4807	0.0171	0.918
Sft-x	0.0110	0.3815	0.5297	0.1074		0.7532	0.1247	1.0000	0.6509	0.0805	0.4527	0.218
Sft-m	0.0213	0.0087	0.3627	0.1855	0.7805		0.1897	0.7321	0.9347	0.1274	0.2498	0.344
R-0	0.4547	0.0226	0.0261	0.7225	0.0992	0.1600		0.0960	0.1257	1.0000	0.0147	0.516
R-x	0.0083	0.3311	0.4647	0.1014	0.0968	0.8265	0.0968		0.6073	0.0516	0.4058	0.167
R-m	0.0009	0.2098	0.2962	0.0507	0.7960	0.9303	0.0681	0.8526		0.0493	0.1158	0.226
Sgm-0	0.3238	0.0120	0.0116	0.6509	0.1793	0.1068	1.0000	0.0544	0.0215		0.0040	0.402
Sgm-x	0.0002	0.7233	1.0000	0.0070	0.9423	0.3039	0.0127	0.4030	0.2004	0.0033		0.009
Sgm-m	0.0866	0.0369	0.0429	0.7432	0.1793	0.2927	0.5502	0.1773	0.1226	0.4592	0.0178	

Table 10: T-test results of GAT models’ performance when training on **BBC** graphs with different combined variants. The bottom and left side measure the accuracy scores, and the top and right side measure the F1 scores on the test set. Statistical significance is highlighted in **bold**.

T-test	Soft-0	Anneal-0	ReLU-0	ReLU-mean	ReLU-max	Sigm-0	Sigm-mean	Sigm-max
Acc	0.0703	0.0017	0.0866	0.8352	0.9342	0.0311	0.2603	0.3109
F1	0.1921	0.0034	0.0989	0.9233	0.8190	0.0494	0.3572	0.2536

Table 11: T-test results of GAT models’ performance when training on **BBC** graphs with different model variants in comparison to the full-attention ReLU baselines. 0 refers to non-filtered graphs. Statistical significance is highlighted in **bold**.

Variant	Ann-0	Ann-x	Ann-m	Sft-0	Sft-x	Sft-m	R-0	R-x	R-m	Sgm-0	Sgm-x	Sgm-m
Ann-0		0.4883	0.4328	0.0042	0.6756	0.7408	0.6259	0.7491	0.4216	0.6857	0.5947	0.5046
Ann-x	0.4697		0.0212	0.1058	0.7681	0.6705	0.7984	0.6402	0.9816	0.7153	0.8704	0.9743
Ann-m	0.4395	0.3083		0.9402	0.7827	0.6561	0.8193	0.3445	0.9100	0.7125	0.9071	0.9696
Sft-0	0.0042	0.1110	0.0212		0.0317	0.1233	0.0286	0.0050	0.0641	0.0124	0.0614	0.0921
Sft-x	0.3833	0.7562	0.8013	0.0309		0.9038	0.9596	0.8769	0.7263	0.9572	0.8975	0.7915
Sft-m	0.7254	0.6574	0.6746	0.0099	0.9017		0.8570	0.9748	0.6142	0.9407	0.8006	0.6927
R-0	0.6043	0.7970	0.8523	0.0309	0.9488	0.8443		0.8268	0.7574	0.9118	0.9330	0.8230
R-x	0.7213	0.6361	0.6434	0.0051	0.8856	0.9871	0.8250		0.5769	0.6152	0.7720	0.6622
R-m	0.4180	1.0000	0.8984	0.0644	0.7319	0.6189	0.7757	0.5918		0.6628	0.8398	0.9534
Sgm-0	0.6954	0.6867	0.7125	0.0124	0.7319	0.9640	0.8787	0.9492	0.6516		0.8498	0.7388
Sgm-x	0.5576	0.8867	0.9584	0.0684	0.8680	0.7687	0.9135	0.7493	0.8762	0.7999		0.8949
Sgm-m	0.4773	0.9827	0.9286	0.0986	0.7705	0.6701	0.8123	0.6484	0.9812	0.7000	0.9027	

Table 12: T-test results of GAT models’ performance when training on **HND** graphs with different combined variants. The bottom and left side measure the accuracy scores, and the top and right side measure the F1 scores on the test set. Statistical significance is highlighted in **bold**.

T-test	Soft-0	Anneal-0	Anneal-max	Anneal-mean	ReLU-0	ReLU-max	ReLU-mean	Sigm-0
Acc	0.0107	0.4728	0.5394	0.3680	0.9069	0.5781	0.7666	0.7646
F1	0.0453	0.5171	0.3680	0.3680	0.8934	0.5697	0.7685	0.7989

Table 13: T-test results of GAT models’ performance when training on **HND** graphs with different model variants in comparison to the full-attention ReLU baselines. 0 refers to non-filtered graphs. Statistical significance is highlighted in **bold**.

Window size	10	20	30	40	50	100
10		0.4866	0.0410	0.0005	0.3058	0.7287
20	0.0480		0.0012	0.0002	0.4909	0.6090
30	0.0527	0.0011		<0.0001	0.0040	0.7336
40	0.0005	0.0002	<0.0001		<0.0001	0.1681
50	0.2743	0.2743	0.0033	<0.0001		0.5534
100	0.2846	0.2328	0.7440	0.0482	0.2073	

Table 14: T-test results of GAT models’ performance when training on **HND** graphs with different window sizes. The bottom and left side measure the accuracy scores, and the top and right side measure the F1 scores on the test set. Statistical significance is highlighted in **bold**.

Variant	Ann-x	Ann-m	Sft-x	Sft-m	R-x	R-m	Sgm-x	Sgm-m
Ann-x		0.13799	0.67630	0.02454	0.62853	0.0702	0.78576	0.12495
Ann-m	0.2197		0.0640	0.0917	0.0621	0.4988	0.2196	0.24149
Sft-x	0.6172	0.0888		0.0115	0.9403	0.0325	0.4934	0.09569
Sft-m	0.0255	0.0938	0.0096		0.0121	0.3587	0.0395	0.33459
R-x	0.5491	0.0776	0.9135	0.0090		0.0323	0.4567	0.09169
R-m	0.0787	0.4020	0.0299	0.4111	0.0269		0.1130	0.28403
Sgm-x	0.7580	0.3850	0.4294	0.0574	0.3785	0.1565		0.14620
Sgm-m	0.0484	0.2317	0.0181	0.6090	0.0166	0.7352	0.1021	

Table 15: T-test results of GAT models’ performance when training on **GR** graphs with different combined variants. The bottom and left side measure the accuracy scores, and the top and right side measure the F1 scores on the test set. Statistical significance is highlighted in **bold**.

T-test	Baselines	ReLU-max	ReLU-mean	Anneal-max	Anneal-mean
Acc	order	0.5205	0.0386	0.9911	0.1478
F1	order	0.4697	0.0507	0.8338	0.8338
Acc	window	0.1194	0.1194	0.7986	0.3245
F1	window	0.1516	0.1516	0.2857	0.2857

Table 16: T-test results of GAT models’ performance when training on **GR** graphs with different model variants in comparison to the full-attention ReLU baselines, as well as heuristic baselines, which previously induced the best performance. Statistic significance is highlighted in **bold**.

D.3 Similarity Scores

We evaluated the predicted summaries using two qualitative text similarity scores, namely ROUGE scores (Lin, 2004) and BERTscore (Zhang et al., 2019). Primarily, ROUGE scores are keyword-based, while BERTScore focuses on semantic similarity but minimal syntactic similarity.

Three ROUGE scores used in this experiment are: ROUGE-1, ROUGE-2, and ROUGE-L; in other words, the overlaps of unigrams, bigrams, and the longest common subsequence, respectively (see Figure 7). The gap between the F1 score, 0.72, and the ROUGE-1 score, 0.33, indicates that the model picks a fairly good number of the oracle sentences, but it might not capture keywords in the exact surface form. In other words, they might suggest that selected sentences differ structurally or positionally from the oracle.

On the other hand, achieving a high BERTScore that also corresponds to accuracy and F1 score shows that the predicted summaries retain high semantic similarity to the oracle summaries. Moreover, a higher ratio of summary sentences (see Section D.2) suggests that GAT models prefer to cover a broader set of sentences that are semantically aligned with the oracle summaries, rather than a handful of densely packed sentences with keywords. In other words, the models appear to favor semantic coverage and topic coherence over purely maximizing lexical overlap. While this strategy may improve the overall quality of representation, it can also lead to lower ROUGE scores.

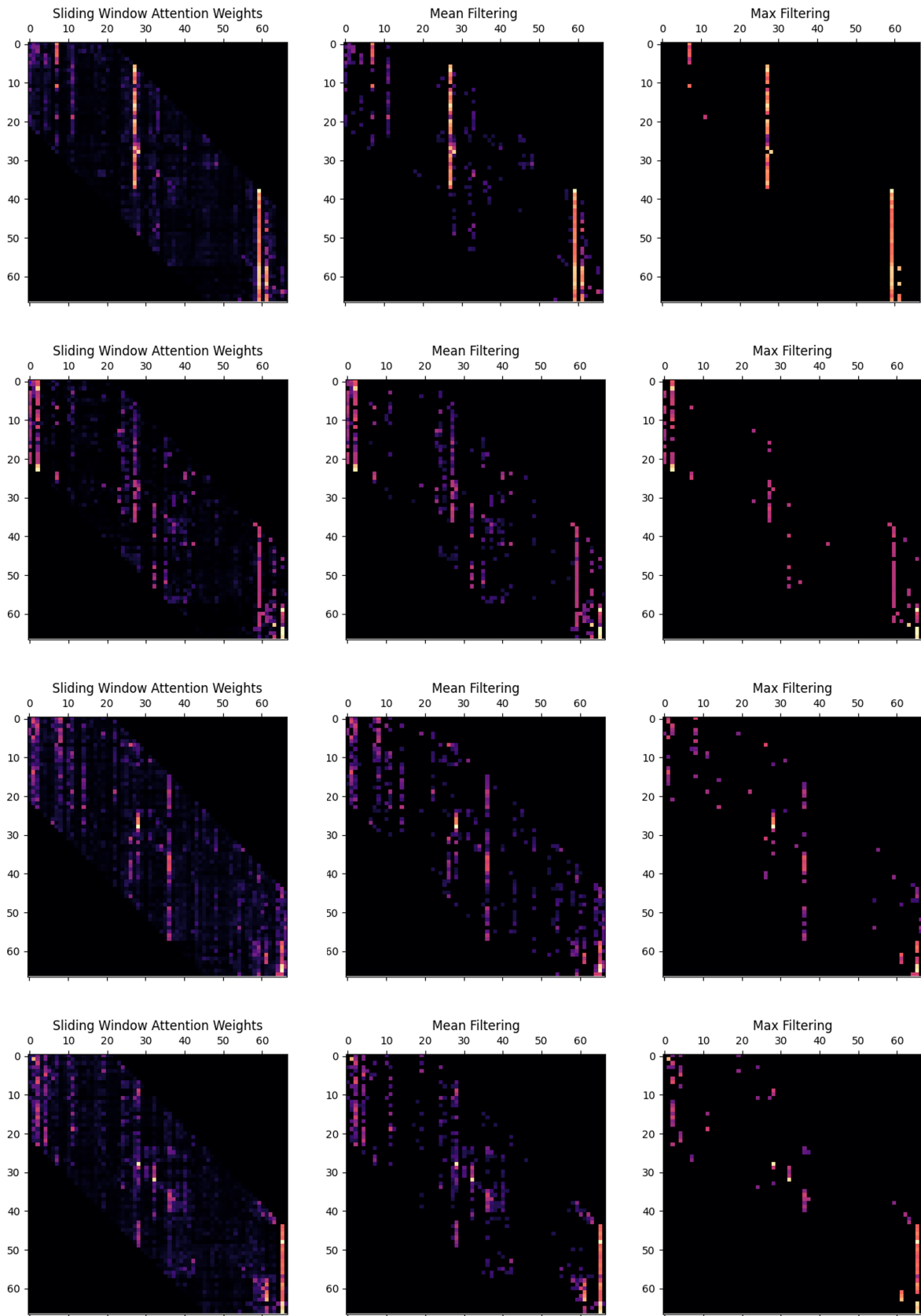


Figure 3: A sample of attention matrices from a randomly selected document in the GovReport dataset. From Top to Bottom: conventional Softmax, Annealing Softmax, ReLU, and Sigmoid. Brighter colors illustrate higher values.

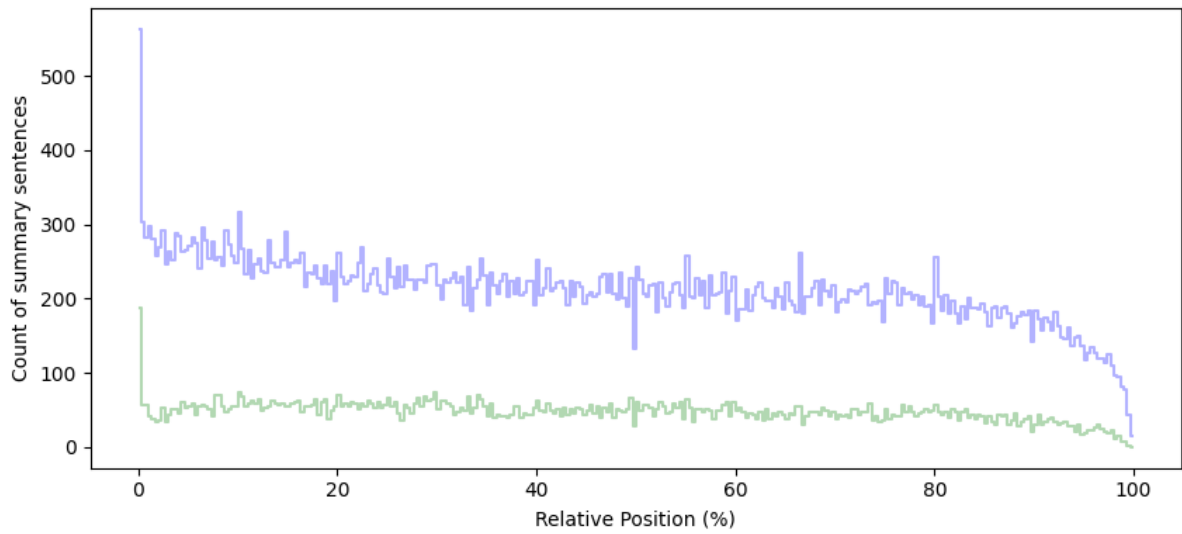


Figure 4: The figure shows the distribution of the summary sentences in relative positions (%) of the documents in the test split. Predicted summary sentences are shown in purple, and oracle summary sentences in green.

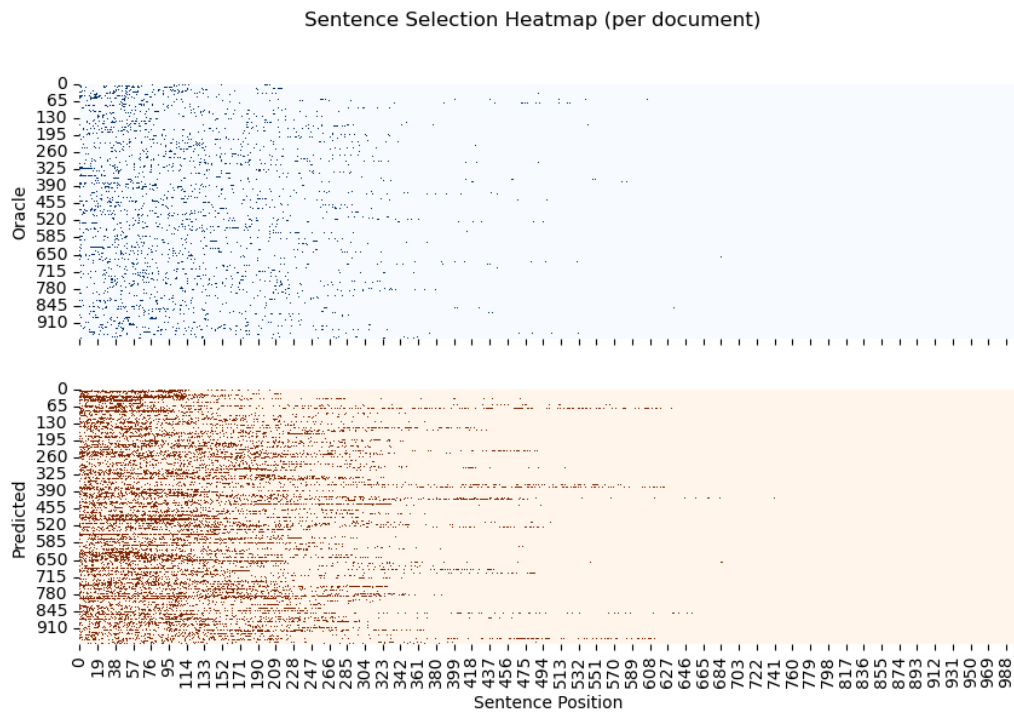


Figure 5: The Figure shows the occurrences of summary sentences from random documents in the test split. Note that the sentence positions are absolute positions with padded length to the 1000th position.

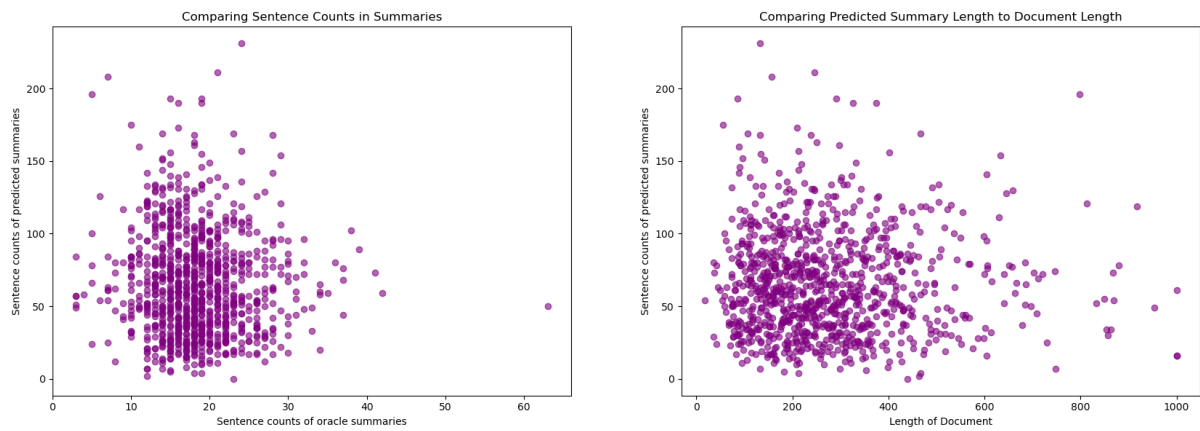


Figure 6: Left: The numbers of Oracle summary sentences (y-axis), compared to the numbers of predicted summary sentences (x-axis). Right: The length of documents (y-axis), compared to the number of predicted summary sentences (x-axis).

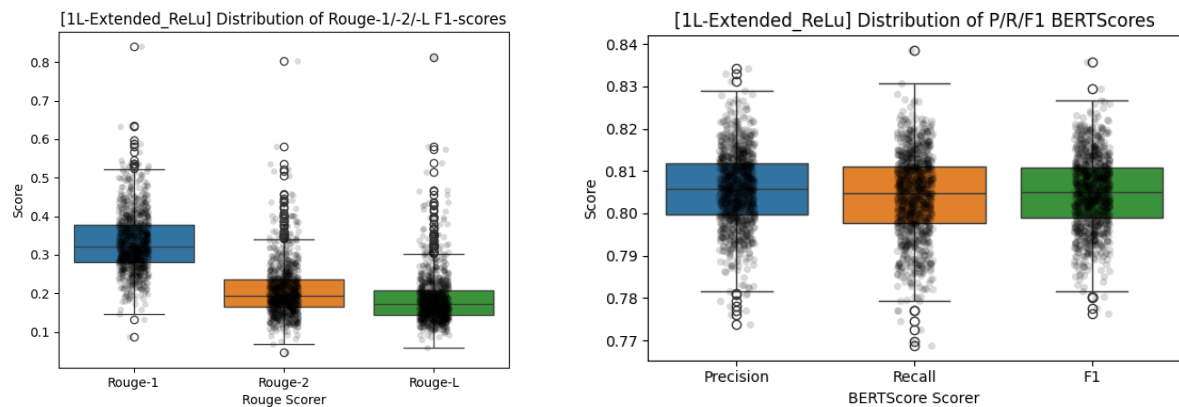


Figure 7: Text similarity scores on summaries generated from the single-layer GAT model trained on ReLU-based graphs. Left: ROUGE-1, ROUGE-2, and ROUGE-L F1 scores on the test split. Right: BERTScore in terms of precision, recall, and F1.